

# Robust Reinforcement Learning in Continuous Control Tasks with Uncertainty Set Regularization

**Yuan Zhang**

Neurorobotics Lab

University of Freiburg

yzhang@cs.uni-freiburg.de

**Jianhong Wang**

Control and Power Research Group

Imperial College London

jianhong.wang16@imperial.ac.uk

**Joschka Boedecker**

Neurorobotics Lab

University of Freiburg

jboedeck@cs.uni-freiburg.de

**Abstract:** Reinforcement learning (RL) is recognized as lacking generalization and robustness under environmental perturbations, which excessively restricts its application for real-world robotics. Prior work claimed that adding regularization to the value function is equivalent to learning a robust policy with uncertain transitions. Although the regularization-robustness transformation is appealing for its simplicity and efficiency, it is still lacking in continuous control tasks. In this paper, we propose a new regularizer named **Uncertainty Set Regularizer (USR)**, by formulating the uncertainty set on the parameter space of the transition function. In particular, USR is flexible enough to be plugged into any existing RL framework. To deal with unknown uncertainty sets, we further propose a novel adversarial approach to generate them based on the value function. We evaluate USR on the Real-world Reinforcement Learning (RWRL) benchmark, demonstrating improvements in the robust performance for perturbed testing environments.

**Keywords:** Reinforcement Learning, Robustness, Robotics

## 1 Introduction

Reinforcement Learning (RL) is a powerful algorithmic paradigm used to solve sequential decision-making problems and has resulted in great success in various types of environments, e.g., mastering the game of GO [1], playing computer games [2] and controlling power systems [3, 4]. The majority of these successes depends on an implicit assumption that *the testing environment is identical to the training environment*. However, this assumption is too strong for most realistic problems, for example, controlling a robot. There are several situations where mismatches might appear between training and testing environments in robotics: (1) *Parameter Perturbations* indicates that a large number of environmental parameters, e.g. temperature, friction factor could fluctuate after deployment and thus deviate from the training environment [5]; (2) *System Identification* estimates a transition function from finite experience. This estimation is biased compared with the real world model [6]; (3) *Sim-to-Real* learns a policy in a simulated environment and performs on real robots for reasons of safety and efficiency [7]. Henceforth, it is essential to develop Robust RL algorithms that can adapt to unseen testing environments for practical applications.

Robust Markov Decision Processes (Robust MDPs) [8, 9] is a common framework for analyzing the robustness of RL algorithms. Compared with regular MDPs with a single transition model  $\mathcal{P}(s'|s, a)$ , Robust MDPs consider an uncertainty set of transition models  $\mathbb{P} = \{\mathcal{P}\}$  to better describe the perturbation of the transitions. This formulation is sufficiently general to cover various scenarios for robot learning problem.

Robust RL aims to learn a robust policy under the worst-case scenario for all transition models  $\mathcal{P} \in \mathbb{P}$ . If the transition model  $\mathcal{P}$  is viewed as an adversarial agent and the uncertainty set  $\mathbb{P}$  is its action space, one can reformulate Robust RL as a zero-sum game [10]. In general, solving such a

problem is NP-hard [9]. Derman et al. [11], however, adopted the Legendre-Fenchel transform to avoid excessive mini-max computations by converting the minimization over the transition model to a regularization on the value function. Furthermore, it enjoys the additional advantage that it provides more possibilities to design novel regularizers for different types of transition uncertainties. Its extension to continuous state space problems (required, e.g., for controlling robots) is unclear, which directly motivates the work of this paper.

In this paper, we (1) extend the robustness-regularization duality method to continuous control tasks; (2) propose the **Uncertainty Set Regularizer (USR)** on existing RL frameworks for learning robust policies; (3) learn an adversarial uncertainty set through the value function when the actual uncertainty set is unknown in some scenarios; (4) evaluate USR on the Real-world Reinforcement Learning (RWRL) benchmark, showing improvements for a robust performance in perturbed testing environments with unknown uncertainty sets.

## 2 Preliminaries

### 2.1 Robust MDPs

The mathematical framework of Robust MDPs [8, 9] extends regular MDPs in order to deal with uncertainty about the transition function. A Robust MDP can be formulated as a 6-tuple  $\langle \mathcal{S}, \mathcal{A}, \mathbb{P}, r, \mu_0, \gamma \rangle$ , where  $\mathcal{S}, \mathcal{A}$  stand for the state and action space respectively, and  $r(s, a) : \mathcal{S} \times \mathcal{A} \rightarrow \mathbb{R}$  stands for the reward function. Let  $\Delta_{|\mathcal{S}|}$  and  $\Delta_{|\mathcal{A}|}$  be the probability measure on  $\mathcal{S}$  and  $\mathcal{A}$  respectively. The initial state is sampled from an initial distribution  $\mu_0 \in \Delta_{\mathcal{S}}$ , and the future rewards are discounted by the discount factor  $\gamma \in [0, 1]$ . The most important concept in robust MDPs is the uncertainty set  $\mathbb{P} = \{\mathcal{P}(s'|s, a) : \mathcal{S} \times \mathcal{A} \rightarrow \Delta_{\mathcal{S}}\}$  that controls the variation of transition  $\mathcal{P}$ , compared with the stationary transition  $\mathcal{P}$  in regular MDPs. Let  $\Pi = \{\pi(a|s) : \mathcal{S} \rightarrow \Delta_{\mathcal{A}}\}$  be the policy space; the objective of Robust RL can then be formulated as a mini-max problem,

$$J^* = \max_{\pi \in \Pi} \min_{\mathcal{P} \in \mathbb{P}} \mathbb{E}_{\pi, \mathcal{P}} \left[ \sum_{t=0}^{+\infty} \gamma^t r(s_t, a_t) \right]. \quad (1)$$

### 2.2 Robust Bellman equation

While Wiesemann et al. [9] has proved NP-hardness of this mini-max problem with an arbitrary uncertainty set, most recent studies [8, 10, 11, 12, 13, 14, 15, 16, 17] approximate it by assuming a rectangular structure on the uncertainty set, i.e.,  $\mathbb{P} = \times_{(s, a) \in \mathcal{S} \times \mathcal{A}} \mathbb{P}_{sa}$ , where  $\mathbb{P}_{sa} = \{\mathcal{P}_{sa}(s') : \Delta_{\mathcal{S}}\}$  denotes the local uncertainty of the transition at  $(s, a)$ . In other words, the variation of transition is independent at every  $(s, a)$  pair. Under the assumption of a rectangular uncertainty set, the robust action value function  $Q^{\pi}(s, a)$  under policy  $\pi$  must satisfy the following robust version of the Bellman equation [18] such that

$$\begin{aligned} Q^{\pi}(s, a) &= r(s, a) + \min_{\mathcal{P}_{sa} \in \mathbb{P}_{sa}} \gamma \sum_{s', a'} \mathcal{P}_{sa}(s') \pi(a'|s') Q^{\pi}(s', a') \\ &= r(s, a) + \min_{\mathcal{P}_{sa} \in \mathbb{P}_{sa}} \gamma \sum_{s'} \mathcal{P}_{sa}(s') V^{\pi}(s'). \end{aligned} \quad (2)$$

Nilim and Ghaoui [12] have shown that a robust Bellman operator admits a unique fixed point of Equation 2, the robust action value function  $Q^{\pi}(s, a)$ .

### 2.3 Robustness-regularization duality

Solving the minimization problem in the RHS of Equation 2 can be further simplified by the Legendre-Fenchel transform [19]. For a function  $f : X \rightarrow \mathbb{R}$ , its convex conjugate is  $f^*(x^*) := \sup \{\langle x^*, x \rangle - f(x) : x \in X\}$ . Define  $\delta_{\mathbb{P}_{sa}}(\mathcal{P}_{sa}) = 0$  if  $\mathcal{P}_{sa} \in \mathbb{P}_{sa}$  and  $+\infty$  otherwise, Equation 2 can be transformed to its convex conjugate (refer Derman et al. [11] for detailed derivation),

$$\begin{aligned} Q^{\pi}(s, a) &= r(s, a) + \min_{\mathcal{P}_{sa}} \gamma \sum_{s'} \mathcal{P}_{sa}(s') V^{\pi}(s') + \delta_{\mathbb{P}_{sa}}(\mathcal{P}_{sa}) \\ &= r(s, a) - \delta_{\mathbb{P}_{sa}}^*(-V^{\pi}(\cdot)). \end{aligned} \quad (3)$$

The transformation implies that the robustness condition on transition can be equivalently expressed as a regularization constraint on the value function, referred to as the robustness-regularization duality. The duality can extensively reduce the cost of solving the minimization problem over infinite transition choices and thus is widely studied in the robust reinforcement learning research community [20, 21, 22].

As a special case, Derman et al. [11] considered a  $L_2$  norm uncertainty set on transitions, i.e.,  $\mathbb{P}_{sa} = \{\bar{\mathcal{P}}_{sa} + \alpha\tilde{\mathcal{P}}_{sa} : \|\tilde{\mathcal{P}}_{sa}\|_2 \leq 1\}$ , where  $\bar{\mathcal{P}}_{sa}$  is usually called the nominal transition model. It could represent prior knowledge on the transition model or a numerical value of the training environment. The uncertainty set denotes that the transition model is allowed to fluctuate around the nominal model with some degree  $\alpha$ . Therefore, the corresponding Bellman equation in Equation 3 becomes  $Q^\pi(s, a) = r(s, a) + \gamma \sum_{s'} \bar{\mathcal{P}}_{sa}(s') V^\pi(s') - \alpha \|V^\pi(\cdot)\|_2$ . Similarly, the  $L_1$  norm has also been used as uncertainty set on transitions [16], i.e.,  $\mathbb{P}_{sa} = \{\bar{\mathcal{P}}_{sa} + \alpha\tilde{\mathcal{P}}_{sa} : \|\tilde{\mathcal{P}}_{sa}\|_1 \leq 1\}$ , and the Bellman equation becomes the form such that  $Q^\pi(s, a) = r(s, a) + \gamma \sum_{s'} \bar{\mathcal{P}}_{sa}(s') V^\pi(s') - \alpha \max_{s'} |V^\pi(s')|$ . This robustness-regularization duality works well with finite state spaces, but is hard to directly extend to infinite state spaces since both  $\|V^\pi(\cdot)\|_2$  and  $\max_{s'} |V^\pi(s')|$  regularizers need calculations on the infinite dimensional vector  $V^\pi(\cdot)$ .

### 3 Uncertainty Set Regularized Robust Reinforcement Learning

Having introduced the robustness-regularization duality and the problems regarding its extension to continuous state space problems in Section 2.3, here, we will first present a novel extension to continuous state space with the uncertainty set defined on the parameter space of the transition function. We will then utilize this extension to derive a robust value iteration that can be directly plugged into existing RL algorithms. Furthermore, to deal with the unknown uncertainty set, we propose an adversarial uncertainty set and visualize it in a simple *moving to target* task.

#### 3.1 Uncertainty Set Regularized Robust Value Iteration (USR-RVI)

For environments with continuous state spaces, the transition model  $\mathcal{P}(s'|s, a)$  is usually represented as a parametric function  $\mathcal{P}(s'|s, a; w)$ , where  $w$  denotes the parameters of the transition function. Instead of defining the uncertainty set on the distribution space, we directly impose a perturbation on  $w$  within a set  $\Omega_w$ . Consequently, the robust objective function (Equation 1) becomes  $J^* = \max_{\pi \in \Pi} \min_{w \in \Omega_w} \mathbb{E}_{\pi, \mathcal{P}(s'|s, a; w)} \left[ \sum_{t=0}^{+\infty} \gamma^t r(s_t, a_t) \right]$ . We further assume the parameter  $w$  fluctuates around a nominal parameter  $\bar{w}$ , such that  $w = \bar{w} + \tilde{w}$ , with  $\bar{w}$  being a fixed parameter and  $\tilde{w} \in \Omega_{\tilde{w}} = \{w - \bar{w} | w \in \Omega_w\}$  being the perturbation part. Inspired by Equation 3, we can derive a robust value iteration algorithm on the parametric space for continuous control problems as shown in Proposition 1.

**Proposition 1** Suppose the uncertainty set of  $w$  is  $\Omega_w$  (i.e., the uncertainty set of  $\tilde{w} = w - \bar{w}$  is  $\Omega_{\tilde{w}}$ ), the robust value iteration on parametric space can be represented as follows:

$$Q^\pi(s, a) = r(s, a) + \gamma \int_{s'} \mathcal{P}(s'|s, a; \bar{w}) V^\pi(s') ds' - \gamma \int_{s'} \delta_{\Omega_{\tilde{w}}}^* [-\nabla_w \mathcal{P}(s'|s, a; \bar{w}) V^\pi(s')] ds', \quad (4)$$

where  $\delta_{\Omega_w}(w)$  is the indicator function that equals 0 if  $w \in \Omega_w$  and  $+\infty$  otherwise, and  $\delta_{\Omega_w}^*(w')$  is the convex dual function of  $\delta_{\Omega_w}(w)$ .

The complete derivation is given in Appendix A.1. Intuitively, Proposition 1 shows that ensuring robustness on parameter  $w$  can be transformed into an additional regularizer on value iteration that relates to the product of the state value function  $V^\pi(s')$  and the derivative of the transition model  $\nabla_w \mathcal{P}(s'|s, a; \bar{w})$ . Taking the  $L_2$  uncertainty set (also used in Derman et al. [11]) as a special case, i.e.,  $\Omega_w = \{\bar{w} + \alpha\tilde{w} : \|\tilde{w}\|_2 \leq 1\}$ , where  $\bar{w}$  stands for the parameter of the nominal transition model  $\mathcal{P}(s'|s, a'; \bar{w})$ , the robust value iteration in Proposition 1 becomes

$$Q^\pi(s, a) = r(s, a) + \gamma \int_{s'} \mathcal{P}(s'|s, a; \bar{w}) V^\pi(s') ds' - \alpha \int_{s'} \|\nabla_w \mathcal{P}(s'|s, a; \bar{w}) V^\pi(s')\|_2 ds'. \quad (5)$$

Following the idea of Q-Learning [23], a Bellman operator can be naturally derived from Equation 5 to learn a robust policy. The two integrals in Equation 5 can be calculated exactly or approximated by sampling methods. We will discuss these in details in the following section.

### 3.2 Uncertainty Set Regularized Robust Reinforcement Learning (USR-RRL)

USR-RVI proposed in the last section naturally applies to model-based RL, as model-based RL learns a point estimate of the transition model  $P(s'|s, a; \bar{w})$  by maximum likelihood approaches [24]. Since calculating the derivatives in USR-RVI is computationally involved, we choose to construct a local transition model with mean and covariance as parameters only (cf. comments in Section 7). Specifically, suppose one can access a triple (state  $s$ , action  $a$  and next state  $s'$ ) from the experience replay buffer, a local transition model  $P(s'|s, a; \bar{w})$  is constructed as a Gaussian distribution with mean  $\bar{w}$  and covariance  $\Sigma$  (with  $\Sigma$  being a hyperparameter), i.e., the nominal parameter  $\bar{w}$  consists of  $(x, \Sigma)$ . With this local transition model, we now have the full knowledge of  $\mathcal{P}(s'|s, a; \bar{w})$  and  $\nabla_w \mathcal{P}(s'|s, a; \bar{w})$ , which allows us to calculate the RHS of Equation 5. To further approximate the integral calculation in Equation 5, we sample  $M$  points  $\{s_1, s_2, \dots, s_M\}$  from the local transition model  $\mathcal{P}(s'|s, a; \bar{w})$  and use them to approximate the target action value function by  $Q^\pi(s, a) \approx r(s, a) + \gamma \sum_{i=1}^M [V^\pi(s_i) - \alpha \|\nabla_w \mathcal{P}(s_i|s, a; \bar{w}) V^\pi(s_i)\|_2 / \mathcal{P}(s_i|s, a; \bar{w})]$ , where  $\bar{w} = (x, \Sigma)$ . With this approximated value iteration, the Bellman operator is guaranteed to converge to the robust value of current policy  $\pi$ . Policy improvement can be further applied to learn a more robust policy.

### 3.3 Adversarial uncertainty set

The proposed method in Section 3.2 relies on the prior knowledge of the uncertainty set of the parameter space. The  $L_p$  norm uncertainty set is most widely used in the Robust RL and robust optimal control literature. However, such a fixed uncertainty set may not sufficiently adapt for various perturbation types. The  $L_p$  norm uncertainty set with its larger region can result in an over-conservative policy, while the one with a smaller region may lead to a risky policy. In this section, we learn an adversarial uncertainty set through the agent's policy (and value function).

The basic idea of the adversarial uncertainty set is to provide a broader uncertainty range to parameters that are more sensitive to the value function, which is naturally measured by the derivative. The agent learning on such an adversarial uncertainty set is easier to adapt to the various perturbation types of parameters. We generate the adversarial uncertainty set in 5 steps as illustrated in Figure 1, (1) *sample* next state  $s'$  according to the distribution  $\mathcal{P}(\cdot|s, a; \bar{w})$ , given the current state  $s$  and action  $a$ ; (2) *forward* pass by calculating the state value  $V(s')$  at next state  $s'$ ; (3) *backward* pass by using the reparameterization trick [25] to compute the derivative  $g(\bar{w}) = \nabla_w V(s'; \bar{w})$ ; (4) *normalize* the derivative by  $d(\bar{w}) = g(\bar{w}) / [\sum_i^W g(\bar{w})_i]^2]^{0.5}$ ; (5) *generate* the adversarial uncertainty set  $\Omega_w = \{\bar{w} + \alpha \tilde{w} : \|\tilde{w}/d(\bar{w})\|_2 \leq 1\}$ .

### 3.4 Visualizing Adversarial Uncertainty Set

To further investigate the characteristics of the adversarial uncertainty set, we visualize it in a simple *moving to target* task: controlling a particle to move towards a target point  $e$  (Figure 2.a). The two-dimensional state  $s$  informs the position of the agent, and the two-dimensional action  $a = (a_1, a_2)$  ( $\|a\|_2 = 1$  is normalized) controls the force in two directions. The environmental parameter  $w = (w_1, w_2)$  represents the contact friction in two directions respectively. The transition function is expressed as  $s' \sim \mathcal{N}(s + (a_1 w_1, a_2 w_2), \Sigma)$ , and the reward is defined by the progress of the distance to the target point minus a time cost:  $r(s, a, s') = d(s, e) - d(s', e) - 2$ . The nominal value  $\bar{w} = (1, 1)$  (Figure 2.b) indicates the equal friction factor in two directions for the training environment. It is easy to conjecture that the optimal action is pointing towards the target point, and the optimal value function  $V^*(s) = -d(s, e)$ .

We visualize the  $L_2$ ,  $L_1$  and the adversarial uncertainty set of the contact friction  $w$  in Figure 2.(b,c,d) respectively, at a specific state  $s = (4, 3)$  and the optimal action  $a^* = (-0.8, -0.6)$ . We can see that compared with the  $L_2$  uncertainty set, the adversarial uncertainty set extends the

perturbation range of the horizontal dimensional parameter since it is more sensitive to the final return. As a result, the agent learning to resist such an uncertainty set is expected to generally perform well on unseen perturbation types, which will be verified in experiments in the next section.

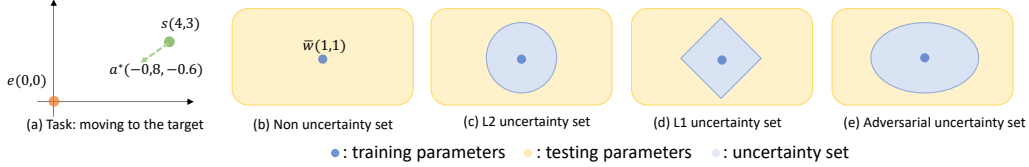


Figure 2: An example of uncertainty set.

## 4 Experiments

In this section, we demonstrate the experimental results on the Real-world Reinforcement Learning (RWRL) benchmark [26], to validate the effectiveness of the proposed regularizing USR for resisting the perturbations in the environment.

### 4.1 Experimental Setups

**Task Description:** RWRL, whose back-end is the Mujoco environment [27]), is a continuous control benchmark consisting of real-world challenges for RL algorithms (e.g., learning from limited samples, dealing with delays in system actuators, high dimensional state and action space). Using this benchmark, we will evaluate the proposed algorithm regarding the robustness of the learned policy in physical environments with perturbations over parameters of the state equations (dynamics). In more detail, we first train a policy through the interaction with the nominal environments (i.e., the environments with no perturbations), and then test the policy in the environments with perturbations within a range over relevant physical parameters.

In this paper, we conduct experiments on six tasks: *cartpole\_balance*, *cartpole\_swingup*, *walker\_stand*, *walker\_walk*, *quadruped\_walk*, *quadruped\_run*, with growing complexity in state and action space. More details about the specifications of tasks are shown in Appendix B.1. The perturbed variables and their value ranges can be found in the Table 2 in Appendix.

**Evaluation metric:** A severe problem for Robust RL research is the lack of a standard metric to evaluate policy robustness. To resolve this obstacle, we define a new robustness evaluation metric which we call *Robust-AUC* to calculate the area under the curve of the return with respect to the perturbed physical variables, in analogy to the definition of regular AUC [28]. More specifically, a policy  $\pi$  after training is evaluated in an environment with perturbed variable  $P$  whose values  $v \in [v_{min}, v_{max}]$  for  $N$  episodes to obtain an  $\alpha$ -percentile return  $r$ . Then, these two sets of data are employed to draw a parameter-return curve  $C(P, R)$  to describe the relationship between returns  $r$  and perturbed values  $v$ . We define the relative area under this curve as Robust-AUC such that  $rv(\pi, P) = \frac{\text{Area}(C(v, r))}{v_{max} - v_{min}}$ ,  $v \in [v_{min}, v_{max}]$ . Compared to the vanilla AUC, Robust-AUC describes the correlation between returns and the perturbed physical variables, which can sensitively reflect the response of a learning procedure (to yield a policy) to the unseen perturbations, i.e., the robustness. In practical implementations, we set  $N = 100$  and  $\alpha = 10$  and uniformly collect 20 samples of  $v$  to estimate the area of the curve.

**Baselines and Implementation of Proposed Methods:** We first compare USR with a standard version of Soft Actor Critic (SAC) [29], which stands for the category of algorithms without regularizers (*None Reg*). Another category of baselines is to directly impose  $L_p$  regularization on the parameters of the value function (*L1 Reg*, *L2 Reg*) [30], which is a common way to improve the generalization of function approximation but without consideration of the environmental perturbations; For a fixed uncertainty set as introduced in Section 3.2, we implement two types of uncertainty sets on transitions, *L2 USR* and *L1 USR*, which can be viewed as an extension of Derman et al. [11] and the work of Wang and Zou [16] work to continuous control task respectively; finally, we also evaluate the adversarial uncertainty set (Section 3.3), denoted as *Adv USR*.

**Experimental Setups:** For a fair comparison, we utilize the same model specifications and hyperparameters for all algorithms in model-free RL and model-based RL respectively, except for the regularizer method and its coefficient. We select the best coefficient for each setting through validation. The detailed model specifications and hyperparameters are shown in Appendix B.3. Each algorithm in the baseline is trained with 5 random seeds. During the test phase, for each environmental variable, we uniformly sample 20 perturbed values  $v$  in the range of  $[v_{min}, v_{max}]$ . For each value  $v$ , we run 20 episodes (5 seeds, in total 100 episodes) and select the 10%-quantile as the return  $r$  to calculate Robust-AUC defined previously.

## 4.2 Main Results

We show the parameter-return curve for all algorithms below in Figure 3 and their Robust-AUC in Table 1. Due to page limits, the results of other tasks are presented in Appendix (Figure 4 and Table 5). In addition to calculating Robust-AUC under different perturbations, we also rank all algorithms and report the average rank as an overall robustness performance of each task. Notably, *L1 Reg* and *L2 Reg* do not improve on the robustness, and even impair the performance in comparison with the non-regularized agent on simple domains (*cartpole* and *walker*). In contrast, we observe that both *L2 USR* and *L1 USR* can outperform the default version under some certain perturbations (e.g. *L1 USR* in *cartpole.swingup* for *pole\_length*, *L2 USR* in *walker\_stand* for *thigh\_length*); they are, however, not effective for all scenarios. We argue that the underlying reason could be that the fixed shape of the uncertainty set cannot adapt to all perturbed cases. This is supported by the fact that *Adv USR* achieves the best average rank among all perturbed scenarios, showing the best zero-shot generalization performance in continuous control tasks.

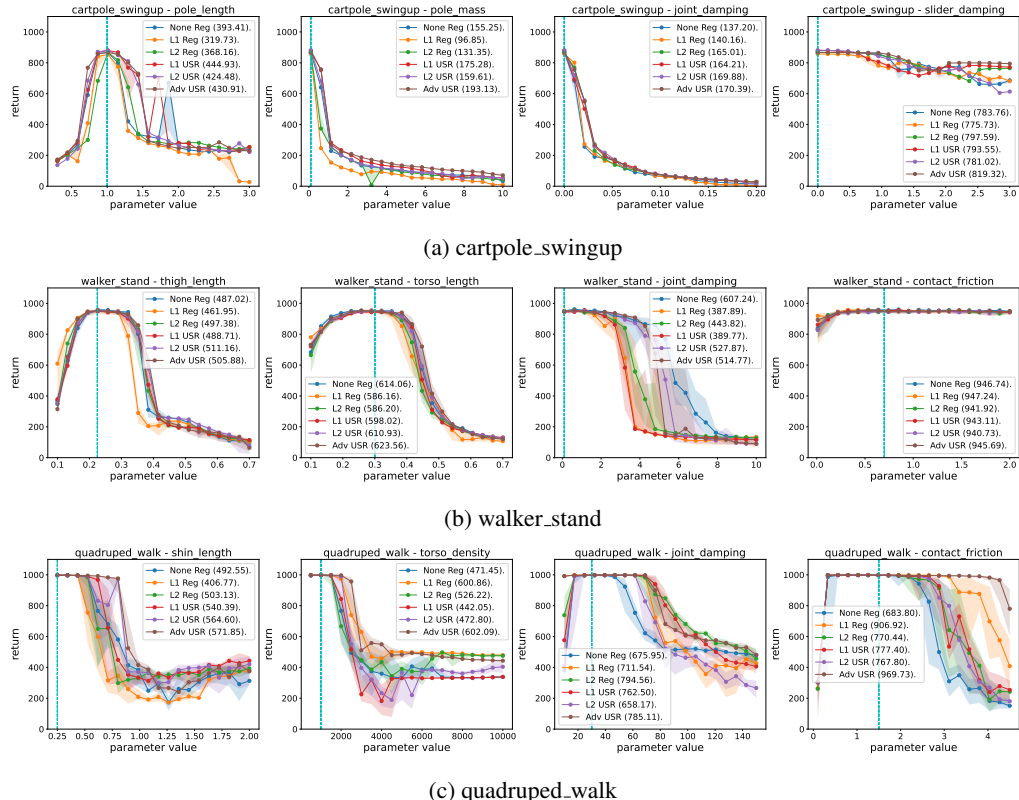


Figure 3: The parameter-return curve of model-free RL algorithms. All graphs are plotted with the 10%-quantile and 5%-15%-quantile shading. The vertical dashed line denotes the nominal value that all algorithms train on. Robust-AUC is illustrated after each label in the graph.

Table 1: Robust-AUC of Model-free RL algorithms.

Task Name	Variables	Algorithms					
		None Reg	L1 Reg	L2 Reg	L1 USR	L2 USR	Adv USR
cartpole.swingup	pole.length	393.41	319.73	368.16	<b>444.93</b>	424.48	430.91
	pole.mass	155.25	96.85	131.35	175.28	159.61	<b>193.13</b>
	joint.damping	137.20	140.16	165.01	164.21	169.88	<b>170.39</b>
	slider.damping	783.76	775.73	797.59	793.55	781.02	<b>819.32</b>
	average rank	4.5	5.75	3.75	2.5	3.25	<b>1.25</b>
walker_stand	thigh.length	487.02	461.95	497.38	488.71	<b>511.16</b>	505.88
	torso.length	614.06	586.16	586.20	598.02	610.93	<b>623.56</b>
	joint.damping	<b>607.24</b>	387.89	443.82	389.77	527.87	514.77
	contact.friction	946.74	<b>947.24</b>	941.92	943.11	940.73	945.69
	average rank	2.50	4.75	4.25	4.25	3.00	<b>2.25</b>
quadruped.walk	shin.length	492.55	406.77	503.13	540.39	564.60	<b>571.85</b>
	torso.density	471.45	600.86	526.22	442.05	472.80	<b>602.09</b>
	joint.damping	675.95	711.54	<b>794.56</b>	762.50	658.17	785.11
	contact.friction	683.80	906.92	770.44	777.40	767.80	<b>969.73</b>
	average rank	5.25	3.50	3.00	3.75	4.25	<b>1.25</b>

## 5 Related Work

Robust Reinforcement Learning (Robust RL) has recently become a popular topic [8, 26, 31, 32], due to its effectiveness in tackling perturbations. Besides the transition perturbation in this paper, there are other branches relating to action, state and reward. We will briefly discuss them in the following paragraphs. Additionally, we will discuss the relation of Robust RL, sim-to-real and Bayesian RL approaches, which are also important topics in robot learning.

**Action Perturbation:** Early works in Robust RL concentrated on action space perturbations. Pinto et al. [33] firstly proposed an adversarial agent perturbing the action of the principle agent, training both alternately in a mini-max style. Tessler et al. [34] later performed action perturbations with probability  $\alpha$  to simulate abrupt interruptions in the real world. Afterwards, Kamalaruban et al. [35] analyzed this mini-max problem from a game-theoretic perspective and claimed that an adversary with mixed strategy converges to a mixed Nash Equilibrium. Similarly, Vinitksy et al. [36] involved multiple adversarial agents to augment the robustness, which can also be explained in the view of a mixed strategy.

**State Perturbation:** State perturbation can lead to the change of state from  $s$  to  $s_p$ , and thus might worsen agent’s policy  $\pi(a|s)$  [37]. Zhang et al. [38], Oikarinen et al. [39] both assume an  $L_p$ -norm uncertainty set on the state space (inspired by the idea of adversarial attacks widely used in computer vision [40]) and propose an auxiliary loss to encourage learning to resist such attacks. It is worth noting that state perturbation is a special case of transition perturbation, and that state perturbations with fixed transitions can be absorbed into transition perturbations, i.e.,  $\mathcal{P}(s'_p|s, a; \bar{w}) = \mathcal{P}(s'|s, a; w)$ , which can be covered by the framework proposed in this paper.

**Reward Perturbation:** The robustness-regularization duality has been widely studied, especially when considering reward perturbations [20, 21, 22]. One reason is that the policy regularizer is closely related to a perturbation on the reward function without the need for a rectangular uncertainty assumption. However, it restricts the scope of these works as reward perturbation, since it can be shown to be a particular case of transition perturbation by augmenting the reward value in the state [21]. Besides, the majority of works focus on the analysis of regularization to robustness, which can only analyze the effect of existing regularizers instead of deriving novel regularizers for robustness as in the work we present here.

**Sim-to-Real:** Sim-to-Real is a key research topic in robot learning. Compared to the Robust RL problem, it aims to learn a robust policy from simulations for generalization in real-world environments. Domain randomization is a common approach to ease this mismatch in sim-to-real problems [41, 7]. However, Mankowitz et al. [14] has demonstrated that it actually optimizes the average case of the environment rather than the worst-case scenario (as seen in our research), which fails to perform robustly during testing. More recent active domain randomization methods [42] resolve this flaw by automatically selecting difficult environments during the training process. The idea of

learning an adversarial uncertainty set considered in this paper can be seen as a strategy to actively search more valuable environments for training.

**Bayesian RL:** One commonality between Bayesian RL and Robust RL is that they both store uncertainties over the environmental parameter (posterior distribution  $q(w)$  in Bayesian RL and uncertainty set  $\Omega_w$  in Robust RL). Uncertainties learned in Bayesian RL can benefit Robust RL in two ways: (1) Robust RL can define an uncertainty set  $\Omega_w = \{w : q(w) > \alpha\}$  to learn a robust policy that can tolerate model errors, which is attractive for offline RL and model-based RL; (2) A soft robust objective with respect to the distribution  $q(w)$  can ease the conservative behaviors caused by the worst-case scenario [15].

## 6 Conclusion

In this paper, we adopt the robustness-regularization duality method to design new regularizers in continuous control problems to improve the robustness and generalization of RL algorithms. Furthermore, to deal with unknown uncertainty sets, we design an adversarial uncertainty set according to the learned action state value function and incorporate it into a new regularizer. While further validation on real world systems is necessary, the proposed method already showed great promise regarding generalization and robustness under environmental perturbations unseen during training, which makes it a valuable addition to RL for robot learning.

## 7 Limitations

The main limitation of the proposed method is possibly the efficiency of the uncertainty set regularizer. Depending on the derivative of the model parameters, it is expensive to compute for environments with a large number of parameters. To address this problem, a workable method is to detect important variables automatically and only apply regularization on these dimensions. Besides, while USR performs well on complex simulated environments in this paper, it should involve more tests on real-world robots in the future.

## Acknowledgments

This research receives funding from the European Union’s Horizon 2020 research and innovation program under the Marie Skłodowska-Curie grant agreement No. 953348 (ELO-X). The authors thank Jasper Hoffman, Baohe Zhang for the inspiring discussions.

## References

- [1] D. Silver, J. Schrittwieser, K. Simonyan, I. Antonoglou, A. Huang, A. Guez, T. Hubert, L. Baker, M. Lai, A. Bolton, Y. Chen, T. Lillicrap, F. Hui, L. Sifre, G. van den Driessche, T. Graepel, and D. Hassabis. Mastering the game of go without human knowledge. *Nature*, 550(7676):354–359, Oct. 2017. ISSN 1476-4687. doi:10.1038/nature24270.
- [2] V. Mnih, K. Kavukcuoglu, D. Silver, A. Graves, I. Antonoglou, D. Wierstra, and M. Riedmiller. Playing atari with deep reinforcement learning, Dec. 2013.
- [3] D. Qiu, J. Wang, J. Wang, and G. Strbac. Multi-agent reinforcement learning for automated peer-to-peer energy trading in double-side auction market. In *IJCAI*, pages 2913–2920, 2021.
- [4] J. Wang, W. Xu, Y. Gu, W. Song, and T. C. Green. Multi-agent reinforcement learning for active voltage control on power distribution networks. *Advances in Neural Information Processing Systems*, 34:3271–3284, 2021.
- [5] J. Kober, J. A. Bagnell, and J. Peters. Reinforcement learning in robotics: A survey. *The International Journal of Robotics Research*, 32(11):1238–1274, 2013.
- [6] S. Schaal. Learning from demonstration. In *Advances in Neural Information Processing Systems*, volume 9. MIT Press, 1996.
- [7] OpenAI, M. Andrychowicz, B. Baker, M. Chociej, R. Jozefowicz, B. McGrew, J. Pachocki, A. Petron, M. Plappert, G. Powell, A. Ray, J. Schneider, S. Sidor, J. Tobin, P. Welinder, L. Weng, and W. Zaremba. Learning dexterous in-hand manipulation, Jan. 2019.
- [8] G. N. Iyengar. Robust dynamic programming. *Mathematics of Operations Research*, 30(2):257–280, May 2005. ISSN 0364-765X, 1526-5471. doi:10.1287/moor.1040.0129.
- [9] W. Wiesemann, D. Kuhn, and B. Rustem. Robust markov decision processes. page 52.
- [10] C. P. Ho, M. Petrik, and W. Wiesemann. Fast bellman updates for robust mdps. In *Proceedings of the 35th International Conference on Machine Learning*, pages 1979–1988. PMLR, July 2018.
- [11] E. Derman, M. Geist, and S. Mannor. Twice regularized mdps and the equivalence between robustness and regularization. In *Advances in Neural Information Processing Systems*, May 2021.
- [12] A. Nilim and L. Ghaoui. Robustness in markov decision problems with uncertain transition matrices. In *Advances in Neural Information Processing Systems*, volume 16. MIT Press, 2004.
- [13] A. Roy, H. Xu, and S. Pokutta. Reinforcement learning under model mismatch. In *Advances in Neural Information Processing Systems*, volume 30. Curran Associates, Inc., 2017.
- [14] D. J. Mankowitz, N. Levine, R. Jeong, A. Abdolmaleki, J. T. Springenberg, Y. Shi, J. Kay, T. Hester, T. Mann, and M. Riedmiller. Robust reinforcement learning for continuous control with model misspecification. In *International Conference on Learning Representations*, Sept. 2019.
- [15] E. Derman, D. J. Mankowitz, T. A. Mann, and S. Mannor. Soft-robust actor-critic policy-gradient. page 11.
- [16] Y. Wang and S. Zou. Online robust reinforcement learning with model uncertainty. In *Advances in Neural Information Processing Systems*, May 2021.

[17] J. Grand-Clément and C. Kroer. Scalable first-order methods for robust mdps. *arXiv:2005.05434 [cs, math]*, Jan. 2021.

[18] R. Bellman. Dynamic programming. *Science*, 153(3731):34–37, July 1966. [doi:10.1126/science.153.3731.34](https://doi.org/10.1126/science.153.3731.34).

[19] R. T. Rockafellar. *Convex Analysis*, volume 18. Princeton university press, 1970.

[20] H. Husain, K. Ciosek, and R. Tomioka. Regularized policies are reward robust. In *Proceedings of The 24th International Conference on Artificial Intelligence and Statistics*, pages 64–72. PMLR, Mar. 2021.

[21] B. Eysenbach and S. Levine. Maximum entropy rl (provably) solves some robust rl problems. In *International Conference on Learning Representations*, Sept. 2021.

[22] R. Brekelmans, T. Genewein, J. Grau-Moya, G. Delétang, M. Kunesch, S. Legg, and P. Ortega. Your policy regularizer is secretly an adversary. *arXiv:2203.12592 [cs, stat]*, Mar. 2022.

[23] R. S. Sutton and A. G. Barto. Reinforcement learning: An introduction. page 352.

[24] B. Kégl, G. Hurtado, and A. Thomas. Model-based micro-data reinforcement learning: What are the crucial model properties and which model to choose? *arXiv:2107.11587 [cs]*, July 2021.

[25] D. P. Kingma and M. Welling. Auto-encoding variational bayes, May 2014.

[26] G. Dulac-Arnold, D. Mankowitz, and T. Hester. Challenges of real-world reinforcement learning. *arXiv:1904.12901 [cs, stat]*, Apr. 2019.

[27] E. Todorov, T. Erez, and Y. Tassa. Mujoco: A physics engine for model-based control. In *2012 IEEE/RSJ International Conference on Intelligent Robots and Systems*, pages 5026–5033, Vilamoura-Algarve, Portugal, Oct. 2012. IEEE. ISBN 978-1-4673-1736-8 978-1-4673-1737-5 978-1-4673-1735-1. [doi:10.1109/IROS.2012.6386109](https://doi.org/10.1109/IROS.2012.6386109).

[28] J. Huang and C. Ling. Using auc and accuracy in evaluating learning algorithms. *IEEE Transactions on Knowledge and Data Engineering*, 17(3):299–310, Mar. 2005. ISSN 1558-2191. [doi:10.1109/TKDE.2005.50](https://doi.org/10.1109/TKDE.2005.50).

[29] T. Haarnoja, A. Zhou, P. Abbeel, and S. Levine. Soft actor-critic: Off-policy maximum entropy deep reinforcement learning with a stochastic actor, Aug. 2018.

[30] Z. Liu, X. Li, B. Kang, and T. Darrell. Regularization matters in policy optimization. Sept. 2019.

[31] R. Kirk, A. Zhang, E. Grefenstette, and T. Rocktäschel. A survey of generalisation in deep reinforcement learning. *arXiv:2111.09794 [cs]*, Jan. 2022.

[32] J. Moos, K. Hansel, H. Abdulsamad, S. Stark, D. Clever, and J. Peters. Robust reinforcement learning: A review of foundations and recent advances. *Machine Learning and Knowledge Extraction*, 4(1):276–315, Mar. 2022. ISSN 2504-4990. [doi:10.3390/make4010013](https://doi.org/10.3390/make4010013).

[33] L. Pinto, J. Davidson, R. Sukthankar, and A. Gupta. Robust adversarial reinforcement learning. *arXiv:1703.02702 [cs]*, Mar. 2017.

[34] C. Tessler, Y. Efroni, and S. Mannor. Action robust reinforcement learning and applications in continuous control. *arXiv:1901.09184 [cs, stat]*, May 2019.

[35] P. Kamalaruban, Y.-T. Huang, Y.-P. Hsieh, P. Rolland, C. Shi, and V. Cevher. Robust reinforcement learning via adversarial training with langevin dynamics. page 12, 2020.

[36] E. Vinitsky, Y. Du, K. Parvate, K. Jang, P. Abbeel, and A. Bayen. Robust reinforcement learning using adversarial populations. *arXiv:2008.01825 [cs, stat]*, Sept. 2020.

[37] A. Pattanaik, Z. Tang, S. Liu, G. Bommannan, and G. Chowdhary. Robust deep reinforcement learning with adversarial attacks. *arXiv:1712.03632 [cs]*, Dec. 2017.

- [38] H. Zhang, H. Chen, C. Xiao, B. Li, M. Liu, D. Boning, and C.-J. Hsieh. Robust deep reinforcement learning against adversarial perturbations on state observations. *arXiv:2003.08938 [cs, stat]*, July 2021.
- [39] T. Oikarinen, W. Zhang, A. Megretski, T.-W. Weng, and L. Daniel. Robust deep reinforcement learning through adversarial loss. page 20, 2021.
- [40] C. Szegedy, W. Zaremba, I. Sutskever, J. Bruna, D. Erhan, I. Goodfellow, and R. Fergus. Intriguing properties of neural networks. *arXiv:1312.6199 [cs]*, Feb. 2014.
- [41] X. B. Peng, M. Andrychowicz, W. Zaremba, and P. Abbeel. Sim-to-real transfer of robotic control with dynamics randomization. In *2018 IEEE International Conference on Robotics and Automation (ICRA)*, pages 1–8. IEEE, 2018.
- [42] B. Mehta, M. Diaz, F. Golemo, C. J. Pal, and L. Paull. Active domain randomization. In *Proceedings of the Conference on Robot Learning*, pages 1162–1176. PMLR, May 2020.
- [43] Y. Tassa, Y. Doron, A. Muldal, T. Erez, Y. Li, D. d. L. Casas, D. Budden, A. Abdolmaleki, J. Merel, A. Lefrancq, T. Lillicrap, and M. Riedmiller. Deepmind control suite. *arXiv:1801.00690 [cs]*, Jan. 2018.
- [44] D. Yarats and I. Kostrikov. Soft actor-critic (sac) implementation in pytorch, 2020.
- [45] H. van Hasselt, A. Guez, and D. Silver. Deep reinforcement learning with double q-learning, Dec. 2015.

## Appendix

### A Extra Algorithm Details

#### A.1 Derivation of Uncertainty Set Regularized Robust Value Iteration

In this section, we will give the proof of Proposition 1. This proposition indicates the transformation from minimization on uncertainty set to regularization on value function, which is the key formulation used in this paper.

**Proposition 1** *Suppose the uncertainty set of  $w$  is  $\Omega_w$  (i.e., the uncertainty set of  $\tilde{w} = w - \bar{w}$  is  $\Omega_{\tilde{w}}$ ), the robust value iteration on parametric space can be represented as follows:*

$$Q^\pi(s, a) = r(s, a) + \gamma \int_{s'} \mathcal{P}(s'|s, a; \bar{w}) V^\pi(s') ds' - \gamma \int_{s'} \delta_{\Omega_{\tilde{w}}}^* [-\nabla_w \mathcal{P}(s'|s, a; \bar{w}) V^\pi(s')] ds' \quad (6)$$

where  $\delta_{\Omega_w}(w)$  is the indicator function that equals 0 if  $w \in \Omega_w$  and  $+\infty$  otherwise, and  $\delta_{\Omega_w}^*(w')$  is the convex dual function of  $\delta_{\Omega_w}(w)$ .

**Proof** The proof is as follows:

$$\begin{aligned} Q^\pi(s, a) &= r(s, a) + \gamma \min_{w \in \Omega_w} \int_{s'} \mathcal{P}(s'|s, a; w) V^\pi(s') ds' \\ &= r(s, a) + \gamma \int_{s'} \mathcal{P}(s'|s, a; \bar{w}) V^\pi(s') ds' + \gamma \min_{w \in \Omega_w} \int_{s'} (w - \bar{w})^T \nabla_w \mathcal{P}(s'|s, a; \bar{w}) V^\pi(s') ds' \\ &= r(s, a) + \gamma \int_{s'} \mathcal{P}(s'|s, a; \bar{w}) V^\pi(s') ds' + \gamma \min_{\tilde{w}} \int_{s'} \tilde{w}^T \nabla_w \mathcal{P}(s'|s, a; \bar{w}) V^\pi(s') ds' + \delta_{\Omega_{\tilde{w}}}(\tilde{w}) \\ &= r(s, a) + \gamma \int_{s'} \mathcal{P}(s'|s, a; \bar{w}) V^\pi(s') ds' - \gamma \left[ \max_{\tilde{w}} \int_{s'} -\tilde{w}^T \nabla_w \mathcal{P}(s'|s, a; \bar{w}) V^\pi(s') ds' - \delta_{\Omega_{\tilde{w}}}(\tilde{w}) \right] \\ &= r(s, a) + \gamma \int_{s'} \mathcal{P}(s'|s, a; \bar{w}) V^\pi(s') ds' - \gamma \int_{s'} \delta_{\Omega_{\tilde{w}}}^* [-\nabla_w \mathcal{P}(s'|s, a; \bar{w}) V^\pi(s')] ds' \end{aligned} \quad (7)$$

The second line utilizes the first-order Taylor Expansion at  $\bar{w}$ . The third line reformulates the minimization on  $w$  to minimization on  $\tilde{w}$  and plus an indicator function as a hard constraint on  $\tilde{w}$ . The forth line changes the minimization to maximization by adding minus symbol in the formulation. The last line directly follows the definition of convex conjugate function.

#### A.2 Uncertainty Set Regularized Robust Soft Actor Critic

The proposed Uncertainty Set Regularizer method is flexible to insert into any existing RL frameworks as introduced in 3.1. Here, we include a specific implementation on Soft Actor Critic algorithm, see Algorithm 1.

## B Extra Experimental Setups

### B.1 RWRL Benchmarks

All tasks in RWRL benchmarks involve a domain and a task. For example, cartpole\_balance represents the balance task on cartpole domain. In this paper, we consider 3 domains with 2 tasks each. The 3 domains are cartpole, walker and quadruped.

**Cartpole:** has an unactuated pole basing on a cart. One can apply a one-direction force to balance the pole. For balance task, the pole starts near the upright while in swingup task the pole starts pointing down.

**Walker:** is a planar walker to be controlled in 6 dimensions. The stand task requires an upright torso and some minimal torso height. The walk task encourages a forward velocity.

---

**Algorithm 1** Uncertainty Set Regularized Robust Soft Actor Critic

---

```

1: Input: initial state  $s$ , action value  $Q(s, a; \theta)$ 's parameters  $\theta_1, \theta_2$ , policy  $\pi(a|s; \phi)$ 's parameters  $\phi$ , replay buffer  $\mathcal{D} = \emptyset$ , transition nominal parameters  $\bar{w}$ , value target update rate  $\rho$ 
2: Set target value parameters  $\theta_{tar,1} \leftarrow \theta_1, \theta_{tar,2} \leftarrow \theta_2$ 
3: repeat
4:   Execute  $a \sim \pi(a|s; \phi)$  in the environment
5:   Observe reward  $r$  and next state  $s'$ 
6:    $\mathcal{D} \leftarrow \mathcal{D} \cup \{s, a, r, s'\}$ 
7:    $s \leftarrow s'$ 
8:   for each gradient step do
9:     Randomly sample a batch transitions,  $\mathcal{B} = \{s, a, r, s'\}$  from  $\mathcal{D}$ 
10:    Construct adversarial adversarial uncertainty set  $\Omega_{\bar{w}}$  as introduced in Section 3.3 (for ad-
        versarial uncertainty set only)
11:    Compute robust value target  $y(s, a, r, s', \bar{w})$  by calculating the RHS of Equation 4
12:    Update action state value parameters  $\theta_i$  for  $i \in \{1, 2\}$  by minimizing mean squared loss to
        the target:
        
$$\nabla_{\theta_i} \frac{1}{|\mathcal{B}|} \sum_{(s, a, r, s') \in \mathcal{B}} (Q(s, a; \theta_i) - y(s, a, r, s', \bar{w}))^2 \quad \text{for } i = 1, 2$$

13:    Update policy parameters  $\phi$  by policy gradient:
        
$$\nabla_{\phi} \frac{1}{|\mathcal{B}|} \sum_{(s) \in \mathcal{B}} (\min_{i=1,2} Q(s, \tilde{a}; \theta_i) - \alpha \log \pi(\tilde{a}|s; \phi))$$

        where  $\tilde{a}$  is sampled from  $\pi(a|s; \phi)$  and differentiable w.r.t.  $\phi$ 
14:    Update target value parameters:
        
$$\theta_{tar,i} \leftarrow (1 - \rho)\theta_{tar,i} + \rho\theta_i \quad \text{for } i = 1, 2$$

15:  end for
16: until convergence

```

---

**Quadruped:** is a generic quadruped with more complex state and action space than cartpole and walker. The walk and run tasks encourage a different level of forward speed.

For detailed description of these tasks and domains, please refer DM control suite [43]. For each task, we follow the RWRL's setup and select 4 environmental variables and perturb them during the testing phase. The perturbed variables and their value ranges can be found in Table 2.

Table 2: Tasks in RWRL benchmark and the perturbed variables

Task Name	Observation Dimension	Action Dimension	Perturbed Variables	Perturbed Range	Nominal Value
cartpole_balance/swingup	5	1	pole_length	[0.3, 3.0]	1.0
			pole_mass	[0.1, 10.0]	0.1
			joint_damping	[2e-6, 2e-1]	2e-6
			slider_damping	[5e-4, 3.0]	5e-4
walker_stand/walk	24	6	tigh_length	[0.1, 0.7]	0.225
			torso_length	[0.1, 0.7]	0.3
			joint_damping	[0.1, 10.0]	0.1
			contact_friction	[0.01, 2.0]	0.7
quadruped_walk/run	78	12	shin_length	[0.25, 2.0]	0.25
			torso_density	[500, 1000]	1000
			joint_damping	[10, 150]	30
			contact_friction	[0.1, 4.5]	1.5

## B.2 Model Structure

The model structure for all experimental baselines is based on the Yarats and Kostrikov [44]'s implementation of Soft Actor Critic (SAC) [29] algorithm. The actor network is a 3-layer feed-forward network with 1024 hidden units and outputs the Gaussian distribution of action. The critic network adopts the double-Q structure [45] and also has 3 hidden layers with 1024 hidden units on each layer, but only outputs a real number as the action state value.

### B.3 Hyperparameters

To compare all algorithms fairly, we set all hyperparameters equally except the robust method and its coefficient. All algorithms are trained with Adam optimizer [25]. The full hyperparameters are shown in Table 3. For regularizer coefficients of all robust update methods, please see Table 4. We can see that this parameter is pretty robust and do not need very handy work to finetune. All experiments are carried out on NVIDIA GeForce RTX 2080 Ti and Pytorch 1.10.1.

Table 3: The hyperparameters of Robust RL algorithms.

HYPERPARAMETERS	VALUE	DESCRIPTION
BATCH SIZE	1024	THE NUMBER OF TRANSITIONS FOR EACH UPDATE
DISCOUNT FACTOR $\gamma$	0.99	THE IMPORTANCE OF FUTURE REWARDS
REPLAY BUFFER SIZE	1e6	THE MAXIMUM NUMBER OF TRANSITIONS STORED IN MEMORY
EPISODE LENGTH	1e3	THE MAXIMUM TIME STEPS PER EPISODE
MAX TRAINING STEP	1e6	THE NUMBER OF TRAINING STEPS
RANDOM STEPS	5000	THE NUMBER OF RANDOMLY ACTING STEPS AT THE BEGINNING
ACTOR LEARNING RATE	1e-4	THE LEARNING RATE FOR ACTOR NETWORK
ACTOR UPDATE FREQUENCY	1	THE FREQUENCY FOR UPDATING ACTOR NETWORK
ACTOR LOG STD BOUNDS	[−5, 2]	THE OUTPUT BOUND OF LOG STANDARD DEVIATION
CRITIC LEARNING RATE	1e-4	THE LEARNING RATE FOR CRITIC NETWORK
CRITIC TARGET UPDATE FREQUENCY	2	THE FREQUENCY FOR UPDATING CRITIC TARGET NETWORK
CRITIC TARGET UPDATE COEFFICIENT	0.005	THE UPDATE COEFFICIENT OF CRITIC TARGET NETWORK FOR SOFT LEARNING
INIT TEMPERATURE	0.1	INITIAL TEMPERATURE OF ACTOR'S OUTPUT FOR EXPLORATION
TEMPERATURE LEARNING RATE	1e-4	THE LEARNING RATE FOR UPDATING THE POLICY ENTROPY
SAMPLE SIZE	1	THE SAMPLE SIZE TO APPROXIMATE THE ROBUST REGULARIZOR

Table 4: The regularizer coefficient of Robust RL algorithms.

Task Name	Algorithms					
	None Reg	L1 Reg	L2 Reg	L1 USR	L2 USR	Adv USR
cartpole_balance	-	1e-5	1e-4	5e-5	1e-4	1e-5
cartpole_swingup	-	1e-5	1e-4	1e-4	1e-4	1e-4
walker_stand	-	1e-4	1e-4	5e-5	1e-4	1e-4
walker_walk	-	1e-4	1e-4	1e-4	1e-4	5e-4
quadruped_walk	-	1e-5	1e-4	1e-4	1e-4	5e-4
quadruped_run	-	1e-4	1e-4	5e-5	1e-4	7e-5

## C Extra Experimental Results

Extra experimental results for task *cartpole\_balance*, *walker\_walk* and *quadruped\_run* can be found in Figure 4 and Table 5. We can observe the similar results as in main paper that both *L2 USR* and *L1 USR* can outperform the default version under some certain perturbations (e.g. *L1 USR* in *cartpole\_balance* for *pole\_mass*, *L2 USR* in *walker\_walk* for *thigh\_length*), while *Adv USR* achieves the best average rank among all perturbed scenarios, showing the best zero-shot generalization performance in continuous control tasks. Notably, *L2 Reg* in *walker\_walk* and *L1 Reg* in *quadruped\_run* also achieve a competitive robust performance compared with *Adv USR*. A possible reason is that, for environment with a high-dimensional state and action spaces, some of them are redundant and direct regularization on value function's parameters is effective to perform dimensionality reduction and thus learns a generalized policy.

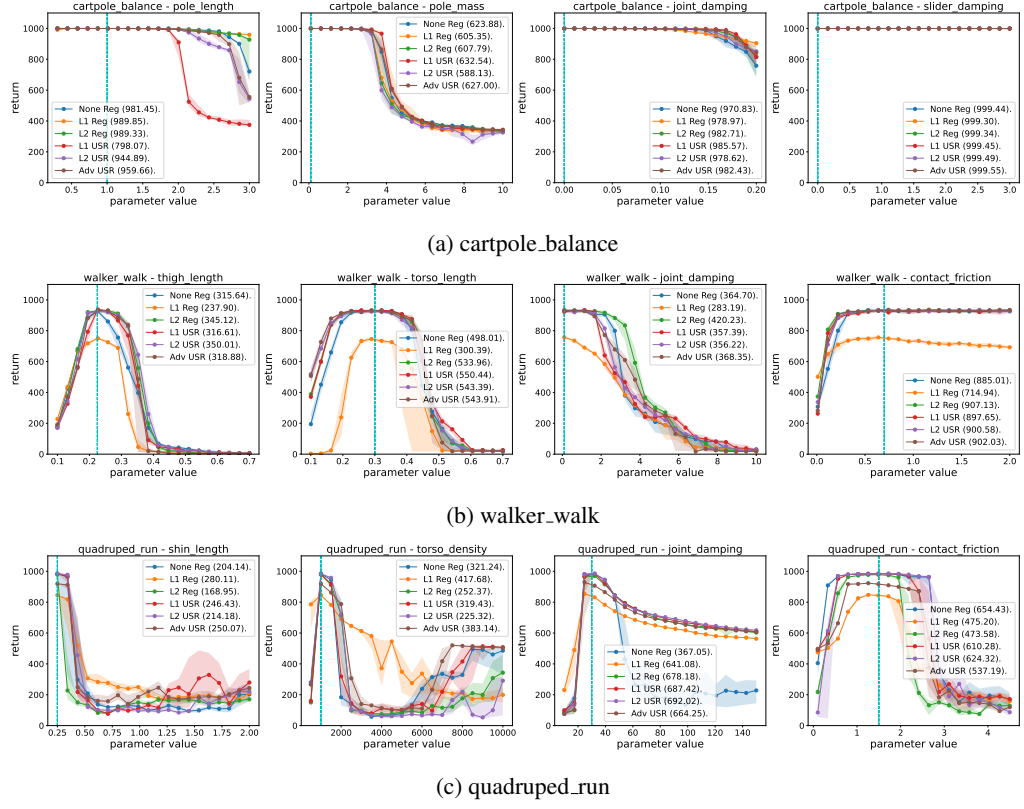


Figure 4: The parameter-return curve of model-free RL algorithms. All graphs are plotted with the 10%-quantile and 5%-15%-quantile shading. The vertical dashed line denotes the nominal value that all algorithms train on. Robust-AUC is illustrated after each label in the graph.

Table 5: Robust-AUC of Model-free RL algorithms.

Task Name	Variables	Algorithms					
		None Reg	L1 Reg	L2 Reg	L1 USR	L2 USR	Adv USR
cartpole_balance	pole_length	981.45	<b>989.85</b>	989.33	798.07	944.89	959.66
	pole_mass	623.88	605.35	607.79	<b>632.54</b>	588.13	627.00
	joint_damping	970.83	978.97	982.71	<b>985.57</b>	978.62	982.43
	slider_damping	999.44	999.30	999.34	999.45	999.49	<b>999.55</b>
	average rank	4.00	4.00	3.25	2.75	4.50	<b>2.50</b>
walker_walk	thigh_length	315.64	237.90	345.12	316.61	<b>350.01</b>	318.88
	torso_length	498.01	300.39	533.96	<b>550.44</b>	543.39	543.91
	joint_damping	364.70	283.19	<b>420.23</b>	357.39	356.22	368.35
	contact_friction	885.01	714.94	<b>907.13</b>	897.65	900.58	902.03
	average	4.50	6.00	<b>2.00</b>	3.25	3.00	2.25
quadruped_run	shin_length	204.14	<b>280.11</b>	168.95	246.43	214.18	250.07
	torso_density	321.24	<b>417.68</b>	252.37	319.43	225.32	383.14
	joint_damping	367.05	641.08	687.42	324.38	<b>692.02</b>	664.25
	contact_friction	<b>654.43</b>	614.21	473.58	632.64	624.32	537.19
	average rank	3.75	<b>3.00</b>	5.00	<b>3.00</b>	3.25	<b>3.00</b>